

# Power and Rate Allocations for Positive-rate Covert Communications in Block-Fading Channels

Yubo Zhang, Hassan ZivariFard, and Xiaodong Wang

**Abstract**— We aim to achieve keyless covert communication with a positive-rate in Rayleigh block-fading channels. Specifically, the transmitter and the legitimate receiver are assumed to have either causal or non-causal knowledge of the channel state information (CSI) for both the legitimate and the warden channels, while the warden only knows the statistical distribution of the CSI. Two problem formulations are considered in this work: (a) Power allocation: maximizing the sum covert rate subject to a maximum power constraint, and (b) Rate allocation: minimizing the power consumption subject to a minimum covert rate constraint. Both problems are formulated based on recent information theoretical results on covert communication over state-dependent channels. When the CSI of each fading block is known non-causally, we propose a novel three-step method to solve both the power and rate allocation problems. In the case where the CSI is known causally, the power allocation problem can be formulated as Markov decision process (MDP) and be solved using a double deep Q-network (DDQN) approach. Although the rate allocation problem under causal CSI does not directly conform to an MDP structure, it can be approximately solved using the DDQN trained for power allocation. Simulation results demonstrate the effectiveness of the proposed power and rate allocation methods and provide comprehensive performance comparisons across different allocation schemes.

**Index Terms**—positive-rate covert communications, block fading channels, non-causal CSI, causal CSI, non-convex optimization, deep Q-learning.

## I. INTRODUCTION

WITH the rapid advancement of next-generation wireless systems, particularly the upcoming sixth-generation (6G) networks, security-related challenges have become increasingly critical and are receiving unprecedented attention [1]. Traditionally, secure information transmission was guarded by physical layer security (PLS) techniques [2], [3], which aim to improve the transmission throughput while ensuring the confidentiality of information. However, in many practical scenarios, it is not only the content of the communication but also its presence that needs to be concealed. To address this concern, covert communication has emerged as a promising paradigm, aiming to hide the act of communication itself from potential adversaries [4], [5].

### A. Information Theoretic Results on Positive-rate Covert Communications

It is well known that, over a point-to-point channel, only  $\mathcal{O}(\sqrt{n})$  bits can be covertly and reliably transmitted in  $n$

channel uses. As a result, the covert rate per channel use approaches zero as  $n \rightarrow \infty$  [4]. To overcome this limitation and achieve a positive covert rate, several enhanced schemes have been proposed. The studies in [6]–[9] leveraged noise uncertainty from the warden’s perspective, allowing  $\mathcal{O}(n)$  bits to be covertly and reliably transmitted over  $n$  channel uses. Meanwhile, the works in [10], [11] showed that a positive covert rate can be achieved when the warden lacks precise knowledge of the transmission time. Furthermore, the application of an uninformed jammer [12], [13] or a cooperative jammer [13], [14] can also enable positive-rate covert communications. In addition, it is shown that the knowledge of the channel state information (CSI) and the knowledge of the action-dependent states can help achieve a positive covert rate [15]–[17]. In [18], a positive covert capacity is achieved over multiple-input multiple-output (MIMO) additive white Gaussian noise (AWGN) channels. Other approaches to achieving a positive covert rate include employing a full-duplex receiver to generate self-interference that impairs the warden’s detection capabilities [19], or adopting multi-hop routing to obscure the transmission source [20].

### B. Optimization of Covert Communications

Recently, the analysis and optimization of covert communications have attracted significant attention. In [21], the transmitter employed channel inversion power control (CIPC) assuming imperfect CSI at both the legitimate receiver and the warden. The fixed received power was optimized to maximize the effective covert throughput. Covert communication over quasi-static fading channels was studied in [22], where channel coefficients are unknown to all terminals and the warden employs a radiometer. The authors derived the optimal transmit power and number of transmit symbols to maximize the covert throughput. Furthermore, covert communication over relay channels — where the relay covertly transmits to the receiver without being detected by the transmitter, has been studied in [23]. The relay’s transmit power was optimized to maximize the effective covert rate under a covert constraint. In [24], covert communication over fading channels is studied and optimized in the presence of a friendly multi-antenna jammer transmitting artificial noise (AN).

In this paper, unlike [21]–[24], we study the covert communication over a point-to-point block-fading channel based on the information theoretic results, and we do not assume the existence of a jammer or relay to assist the transmitter. Motivated by the substantial body of work on rate-maximization [21], [22] and power-minimization [25], [26] in block-fading

The authors are with the Department of Electrical Engineering, Columbia University, New York, NY 10027. E-mails: {yz4891,hz2863,xw2008}@columbia.edu.

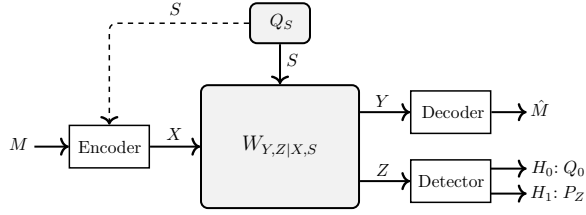


Fig. 1: Covert communication over DMCs.

channels, we formulate and tackle both problems in the context of covert communications in this paper.

### C. Contributions and Outline

Of particular relevance to this paper, [16] characterizes the covert capacity of discrete memoryless channels (DMCs) when the CSI is available either non-causally or causally at both the transmitter and the receiver. In this paper, we study covert communication with positive rates over block-fading channels, building on the results presented in [16]. To the best of our knowledge, the present paper is the first to analyze and optimize keyless covert communications over fading channels. The main contributions of this paper are summarized as follows:

- Building on the results of [16], we formulate non-convex power allocation optimization problems for achieving maximum positive covert rates with a fixed power budget, as well as non-convex rate allocation optimization problems for achieving a fixed positive covert rate with minimum power consumption, under both non-causal and causal CSI at the transmitter.
- When the CSI is known non-causally at the transmitter, a novel three-step method is proposed to solve the power allocation problem, and another fundamentally different three-step method to solve the rate allocation problem. Extensive simulation results are provided to illustrate the effectiveness of the proposed approaches in solving the non-convex power/rate allocation problems.
- When the CSI is known causally at the transmitter, the corresponding power allocation problem is formulated as a MDP and solved using a deep reinforcement learning (DRL) approach. On the other hand, the rate allocation problem is not Markovian, thereby is approximately transformed into a power allocation problem and then solved using the aforementioned DRL method.

The remainder of this paper is organized as follows. In Section II, we introduce the system model and problem formulations. In Section III, we develop algorithms to solve the power and rate allocation problems when the CSI is known non-causally at the legitimate terminals. In Section IV, we develop DRL methods to solve the causal versions of the power and rate allocation problems. Simulation results are presented in Section V, and Section VI concludes the paper.

## II. SYSTEM MODEL AND PROBLEM FORMULATIONS

### A. System Model

Consider the problem of covert communication over block-fading channels with a channel coherence interval of  $T$  sym-

bols. The received signals at the legitimate receiver and the warden, respectively, are

$$Y_\ell(t) = H_\ell X_\ell(t) + N_\ell(t), \quad (1a)$$

$$Z_\ell(t) = G_\ell X_\ell(t) + V_\ell(t), \quad t \in [T] \text{ and } \ell \in [L], \quad (1b)$$

where we assume the length of the codeword is  $LT$ , i.e., the codeword spans over  $L$  coherence blocks;  $X_\ell(t)$  is the  $t^{\text{th}}$  symbol during the  $\ell^{\text{th}}$  coherence block;  $H_\ell \in \mathbb{C}$  and  $G_\ell \in \mathbb{C}$  denote the legitimate receiver's and the warden's channel gains, respectively, during the  $\ell^{\text{th}}$  coherence block, that are circularly symmetric complex Gaussian (CSCG) random variables;  $N_\ell(t) \sim \mathcal{CN}(0, \sigma_n^2)$  and  $V_\ell(t) \sim \mathcal{CN}(0, \sigma_v^2)$  are the additive noise samples at the legitimate receiver and the warden, respectively. Our goal is to design a transmission scheme to maximize the rate at the legitimate receiver while keeping the warden unaware of the transmission.

### B. Problem Formulation Based on Information Theoretic Results

Fig. 1 is a schematic diagram of covert communication over DMC, when the channel state is available at both the transmitter and the receiver but not at the warden, which is studied in [16, Sec. IV]. In Fig. 1,  $M$  is the transmitter's message,  $X \in \mathcal{X}$  is the channel input,  $Y \in \mathcal{Y}$  and  $Z \in \mathcal{Z}$  are the channel outputs of the legitimate receiver and the warden, respectively,  $S \in \mathcal{S}$  is the channel state, and  $W_{Y,Z|X,S}$  is the channel transition probability. Here, the channel state is independent and identically distributed (i.i.d.) and drawn according to  $Q_S$  and we let  $x_0 \in \mathcal{X}$  be an "innocent" symbol corresponding to the absence of communication with the receiver. The distribution induced at the warden in the absence of communication is  $Q_0(\cdot) = \sum_{s \in \mathcal{S}} Q_S(s) W_{Z|X,S}(\cdot|x_0, s)$ . On the other hand, the distribution induced at the output of the warden by the code design is  $P_Z(z) = \sum_{s \in \mathcal{S}} \sum_{x \in \mathcal{X}} \sum_{y \in \mathcal{Y}} Q_S(s) P_{X|S}(x|s) W_{Y,Z|S,X}(y, z|x, s)$ . The legitimate receiver outputs the decoded message  $\hat{M}$  based on the channel output  $Y$ ; whereas the warden attempts to detect the communication by performing a binary hypothesis test between the two distributions  $Q_0^{\otimes n}$  and  $P_Z^n$ , corresponding to the absence and presence of communication, respectively. In covert communication, the transmitter aims to communicate with the receiver both reliably and covertly. Reliable means that the probability of error  $P_e^{(n)} = \mathbb{P}(\hat{M} \neq M)$  vanishes when the codeword length  $n \rightarrow \infty$ . Covert means that the warden cannot determine whether communication is happening (hypothesis  $H_1$ ) or not (hypothesis  $H_0$ ). Specifically, the probability of error of the optimal hypothesis test by the warden is lower bounded by  $1 - \sqrt{\mathbb{D}(P_Z^n || Q_0^{\otimes n})}$  [27]. Therefore, the code is covert if  $\mathbb{D}(P_Z^n || Q_0^{\otimes n})$  vanishes when  $n \rightarrow \infty$ . From [16, Theorem 1] the following rate is achievable for DMCs,

$$\max_{P_{X|S}} \quad I(X; Y|S), \quad (2a)$$

$$\text{s.t.} \quad P_Z = Q_0, \quad (2b)$$

$$I(X; Y|S) \geq I(X; Z|S). \quad (2c)$$

To apply the result in (2) to the block-fading channel defined in (1), we let  $X \leftarrow \{X_\ell\}_{\ell \in [L]}$ ,  $Y \leftarrow \{Y_\ell\}_{\ell \in [L]}$ , and  $S \leftarrow \{(H_\ell, G_\ell)\}_{\ell \in [L]}$ . Assuming that the total power of a codeword is  $P_0$ , and the channel instantaneous SNRs are  $h_\ell \triangleq \frac{|H_\ell|^2}{\sigma_n^2}$  and  $g_\ell \triangleq \frac{|G_\ell|^2}{\sigma_n^2}$ . We make the following assumptions:

- (i) Gaussian signaling:  $X_\ell(t) \sim \mathcal{CN}(0, P_\ell)$ , for  $\ell \in [L]$ , with  $\sum_{\ell=1}^L P_\ell \leq P_0$ .
- (ii) Quantized channel SNRs: the constraint  $I(X; Y|S) \geq I(X; Z|S)$  in (2) implies that we can achieve a positive covert rate only when the legitimate receiver's channel is less noisy than the warden's channel, which is obtained based on the assumption that  $S$  is a discrete random variable. Therefore, we assume that the channel SNRs  $\{h_\ell, g_\ell, \ell \in [L]\}$  are quantized. Such quantization is also needed when we formulate the problem under causal CSI as an MDP. Since the number of quantization levels can be arbitrarily large, the quantized system well approximates the original system.
- (iii) Relaxed covertness constraint: assuming the innocent symbol  $x_0 = 0$ , which is the symbol transmitted by the transmitter in the no communication mode, then the constraint  $P_Z = Q_0$  in (2) becomes  $g_\ell P_\ell = 0$ , for  $\ell \in [L]$ , leading to the trivial solution of  $P_\ell = 0$ . Therefore, we relax this constraint to  $g_\ell P_\ell \leq \epsilon$ .

Then the mutual information terms in (2) become  $I(X; Y|S) = \sum_{\ell=1}^L \log(1 + h_\ell P_\ell)$  and  $I(X; Z|S) = \sum_{\ell=1}^L \log(1 + g_\ell P_\ell)$ . Hence the achievable rate in (2) leads to the following power allocation problem

$$\max_{P_1, \dots, P_L} \sum_{\ell=1}^L \log(1 + h_\ell P_\ell), \quad (3a)$$

$$\text{s.t.} \quad \sum_{\ell=1}^L P_\ell \leq P_0, \quad (3b)$$

$$g_\ell P_\ell \leq \epsilon, \ell \in [L], \quad (3c)$$

$$\sum_{\ell=1}^L \log(1 + h_\ell P_\ell) \geq \sum_{\ell=1}^L \log(1 + g_\ell P_\ell). \quad (3d)$$

The above formulation maximizes the achievable covert rate under a maximum power constraint. Formulation (3) is a non-convex optimization problem due to the less noisy constraint (3d). An alternative formulation is to minimize the total transmit power subject to a minimum covert rate constraint. In particular, let  $R_\ell = \log(1 + h_\ell P_\ell)$ . Then  $P_\ell = \frac{e^{R_\ell} - 1}{h_\ell}$  and we can convert (3) to the following rate allocation problem

$$\min_{R_1, \dots, R_L} \sum_{\ell=1}^L \frac{e^{R_\ell} - 1}{h_\ell}, \quad (4a)$$

$$\text{s.t.} \quad \sum_{\ell=1}^L R_\ell \geq R_0, \quad (4b)$$

$$(e^{R_\ell} - 1) \frac{g_\ell}{h_\ell} \leq \epsilon, \ell \in [L], \quad (4c)$$

$$\sum_{\ell=1}^L R_\ell \geq \sum_{\ell=1}^L \log \left( (e^{R_\ell} - 1) \frac{g_\ell}{h_\ell} + 1 \right). \quad (4d)$$

Here (4a) and (4b) correspond to the minimum total power objective and the minimum covert rate constraint, respectively; (4c) and (4d) are the same covertness constraints as (3c) and (3d), respectively.

In the following sections, we will solve the above two formulations under the following two scenarios:

- (i) Non-causal CSI:  $\{(H_\ell, G_\ell)\}_{\ell \in [L]}$  is available at the beginning of the first block. Then by solving the optimization problem in (3) or (4), we obtain the power or rate allocation for the entire codeword over  $L$  coherence blocks. Note that another scenario that fits such non-causal CSI is the parallel channel setup, where  $\ell$  denotes the sub-channel (e.g., OFDM subcarrier) of the same coherence block.
- (ii) Causal CSI: In this case, at the beginning of the  $\ell^{\text{th}}$  block, for  $\ell \in [L]$ , only  $\{(H_1, G_1), \dots, (H_\ell, G_\ell)\}$  is available, and we need to determine the power allocation  $P_\ell$  and rate allocation  $R_\ell$  sequentially.

### III. POWER AND RATE ALLOCATIONS WITH NON-CAUSAL CSI

In this section, we assume that the channel gains are known non-causally at both the transmitter and legitimate receiver and solve the two non-convex optimization problems in (3) and (4).

#### A. Power Allocation Under Non-causal CSI

We first consider the power allocation problem in (3) for maximum covert sum rate under non-causal CSI. The solution consists of three steps:

- (1) First we check the feasibility of achieving positive covert rate.
- (2) If the problem is feasible, then we will drop the non-convex less noisy constraint and solve the resulting convex problem. If the solution satisfies the less noisy constraint, then it is the optimal solution to the original problem.
- (3) Otherwise we convert the less noisy constraint to a penalty term and add it to the objective function, and optimize it using the projected gradient ascent method, starting from the convex solution in step (2).

1) *Feasibility check*: The non-convex optimization problem in (3) has a positive solution if and only if

$$\exists \ell \in [L] : h_\ell \geq g_\ell. \quad (5)$$

To see the sufficiency, denote  $\mathcal{L} = \{\ell \in [L] : h_\ell \geq g_\ell\}$ . Then the following solution satisfies all constraints in (3b), (3c) and (3d):

$$P_\ell = \begin{cases} \frac{\alpha \epsilon}{g_\ell}, & \ell \in \mathcal{L}, \\ 0, & \ell \notin \mathcal{L}, \end{cases} \quad \text{with } \alpha = \min \left\{ 1, \frac{P_0}{\sum_{\ell \in \mathcal{L}} \frac{\epsilon}{g_\ell}} \right\}. \quad (6)$$

On the other hand, to see the necessity, suppose that (5) does not hold, such that  $h_\ell < g_\ell, \forall \ell \in [L]$ . Then to meet the constraint in (3d) we have  $P_\ell = 0, \forall \ell \in [L]$ , and hence the covert rate is zero.

2) *Convex Power Allocation*: If the problem is feasible, we drop the less noisy constraint in (3d) and solve the resulting convex problem. In particular, we form the Lagrangian

$$\mathcal{L}(\mathbf{P}, \lambda, \boldsymbol{\mu}) = \sum_{\ell=1}^L \log(1 + h_\ell P_\ell) - \lambda \left( \sum_{\ell=1}^L P_\ell - P_0 \right) - \sum_{\ell=1}^L \mu_\ell (g_\ell P_\ell - \epsilon), \quad (7)$$

where  $\mathbf{P} = [P_1, \dots, P_L]$  and  $\boldsymbol{\mu} = [\mu_1, \dots, \mu_L]$ . Since  $P_\ell \geq 0$ ,  $\ell \in [L]$ , we write down the Karush-Kuhn-Tucker (KKT) conditions as follows:

$$\frac{\partial \mathcal{L}(\mathbf{P}, \lambda, \boldsymbol{\mu})}{\partial P_\ell} \leq 0 \Rightarrow P_\ell \geq \frac{1}{\lambda + \mu_\ell g_\ell} - \frac{1}{h_\ell}, \quad \ell \in [L], \quad (8a)$$

$$\left( \frac{\partial \mathcal{L}(\mathbf{P}, \lambda, \boldsymbol{\mu})}{\partial P_\ell} \right) P_\ell = 0 \Rightarrow \left( \frac{1}{P_\ell + \frac{1}{h_\ell}} - \lambda - \mu_\ell g_\ell \right) P_\ell = 0, \quad \ell \in [L], \quad (8b)$$

$$\sum_{\ell=1}^L P_\ell - P_0 \leq 0, \quad \lambda \geq 0, \quad \lambda \left( \sum_{\ell=1}^L P_\ell - P_0 \right) = 0, \quad (8c)$$

$$g_\ell P_\ell - \epsilon \leq 0, \quad \mu_\ell \geq 0, \quad \mu_\ell (g_\ell P_\ell - \epsilon) = 0, \quad \ell \in [L]. \quad (8d)$$

If  $P_\ell = 0$ , from (8d)  $\mu_\ell = 0$ . Hence by (8a)  $\frac{1}{\lambda} - \frac{1}{h_\ell} \leq 0$ . On the other hand, if  $P_\ell > 0$ , from (8b)  $P_\ell = \frac{1}{\lambda + \mu_\ell g_\ell} - \frac{1}{h_\ell}$ . Since  $\mu_\ell \geq 0$ ,  $\frac{1}{\lambda} \geq \frac{1}{\lambda + \mu_\ell g_\ell} > \frac{1}{h_\ell}$ . Therefore

$$P_\ell = \begin{cases} 0, & \frac{1}{\lambda} \leq \frac{1}{h_\ell}, \\ \frac{1}{\lambda + \mu_\ell g_\ell} - \frac{1}{h_\ell}, & \frac{1}{\lambda} > \frac{1}{h_\ell}. \end{cases} \quad (9)$$

Furthermore, if  $\mu_\ell > 0$ , from (8d),  $P_\ell = \frac{\epsilon}{g_\ell}$ . And by (8a)  $P_\ell < \frac{1}{\lambda} - \frac{1}{h_\ell}$ . Hence we have  $\frac{1}{\lambda} > \frac{\epsilon}{g_\ell} + \frac{1}{h_\ell}$ . On the other hand, if  $\mu_\ell = 0$ , by (8a)  $P_\ell = \frac{1}{\lambda} - \frac{1}{h_\ell}$  and by (8d)  $P_\ell \leq \frac{\epsilon}{g_\ell}$ . Hence we have  $\frac{1}{\lambda} \leq \frac{\epsilon}{g_\ell} + \frac{1}{h_\ell}$ . Combining these with (9) and denoting  $\zeta = \frac{1}{\lambda}$ , we have

$$P_\ell^{\text{KKT}} = \begin{cases} 0, & 0 < \zeta \leq \frac{1}{h_\ell}, \\ \zeta - \frac{1}{h_\ell}, & \frac{1}{h_\ell} < \zeta \leq \frac{\epsilon}{g_\ell} + \frac{1}{h_\ell}, \\ \frac{\epsilon}{g_\ell}, & \zeta > \frac{\epsilon}{g_\ell} + \frac{1}{h_\ell}. \end{cases} \quad (10)$$

Now by (8c), if  $\lambda > 0$ ,  $\sum_{\ell=1}^L P_\ell = P_0$ , where  $P_\ell$  is given by (10); and if  $\lambda = 0$ ,  $\sum_{\ell=1}^L P_\ell \leq P_0$ , and by (10),  $P_\ell = \frac{\epsilon}{g_\ell}$ .

Finally based on the above analysis, the convex power allocation  $\mathbf{P}^{\text{KKT}}$  is summarized as follows: If  $\sum_{\ell=1}^L \frac{\epsilon}{g_\ell} \leq P_0$ , then  $P_\ell^{\text{KKT}} = \frac{\epsilon}{g_\ell}$ ,  $\ell \in [L]$ ; otherwise  $\mathbf{P}^{\text{KKT}}$  is given by (10), where  $\zeta > 0$  is chosen such that  $\sum_{\ell=1}^L P_\ell^{\text{KKT}} = P_0$ . If  $\mathbf{P}^{\text{KKT}}$  satisfies the less noisy constraint (3d), then it is the optimal solution to the original problem in (3). Otherwise, in the last step we use the projected gradient ascent method to solve the non-convex optimization problem in (3), starting from  $\mathbf{P}^{\text{KKT}}$ .

3) *Projected gradient ascent*: Define

$$\Delta(\mathbf{P}) = \sum_{\ell=1}^L \log(1 + P_\ell h_\ell) - \sum_{\ell=1}^L \log(1 + P_\ell g_\ell). \quad (11)$$

Then the less noisy constraint in (3d) becomes  $\Delta(\mathbf{P}) \geq 0$ .

Using the penalty method, we convert the convex constraint in (3d) to a penalty term to form the following penalized objective function to be maximized

$$\mathcal{F}(\mathbf{P}, \eta, b) = \sum_{\ell=1}^L \log(1 + P_\ell h_\ell) - \eta \left[ \Delta(\mathbf{P}) - b \right]^2, \quad (12)$$

where  $\eta > 0$  is the penalty factor and  $b \geq 0$  is an auxiliary variable.

The constraints in (3b) and (3c) form a convex feasible set

$$\mathcal{P} = \left\{ \mathbf{P} \mid 0 \leq P_\ell \leq \frac{\epsilon}{g_\ell}, \quad \ell \in [L], \quad \sum_{\ell=1}^L P_\ell \leq P_0 \right\}. \quad (13)$$

In general, to ensure that the original objective function is sufficiently maximized, the penalty factor  $\eta$  should be initialized with a large value. Then it will be gradually increased to guarantee that the penalty term approaches zero. In our case, however, if we initialize as  $\mathbf{P}^{(0)} = \mathbf{P}^{\text{KKT}}$ ,  $\ell \in [L]$ , and  $b^{(0)} = 0$ , then effectively we start from the maximum of the original objective, which is infeasible, i.e.,  $\Delta(\mathbf{P}^{\text{KKT}}) < 0$ . Hence we can initialize  $\eta$  as

$$\eta_0 = \frac{C}{\Delta^2(\mathbf{P}^{(0)})} \sum_{\ell=1}^L \log(1 + P_\ell^{(0)} h_\ell), \quad (14)$$

where  $C \gg 1$  is a constant, so that the initial penalized objective is  $(1 - C) \sum_{\ell=1}^L \log(1 + P_\ell^{(0)} h_\ell) \ll 0$ . Since the original problem in (3) is feasible, there is a solution in  $\mathcal{P}$  with positive penalized objective. Then we apply the following projected gradient ascent (PGA) procedure: for  $n = 0, 1, \dots$ ,

$$\begin{aligned} \mathbf{P}^{(n+1)} &= \Pi_{\mathcal{P}} \left[ \mathbf{P}^{(n)} + \alpha_1 \nabla_{\mathbf{P}} \mathcal{F} \right] \Big|_{\mathbf{P}=\mathbf{P}^{(n)}}, \\ b^{(n+1)} &= \Pi_{\mathbb{R}^+} \left[ b^{(n)} + \alpha_2 \frac{\partial \mathcal{F}}{\partial b} \right] \Big|_{b=b^{(n)}}, \end{aligned} \quad (15)$$

where  $\alpha_1$  and  $\alpha_2$  are step-size parameters,  $\Pi_{\mathcal{P}}$  is a projector onto the feasible set  $\mathcal{P}$  in (13), and  $\Pi_{\mathbb{R}^+}$  is a projector onto the positive real number field, i.e.,  $\Pi_{\mathbb{R}^+}(b) = \max\{b, 0\}$ . For the projector  $\Pi_{\mathcal{P}}$ , note that  $\mathcal{P}$  is an intersection of two convex sets, i.e.,  $\mathcal{P} = \mathcal{P}_1 \cap \mathcal{P}_2$ , where  $\mathcal{P}_1 = \{\mathbf{P} \mid 0 \leq P_\ell \leq \frac{\epsilon}{g_\ell}\}$  and  $\mathcal{P}_2 = \{\mathbf{P} \mid \sum_{\ell=1}^L P_\ell \leq P_0\}$ . Then  $\Pi_{\mathcal{P}}(\mathbf{P})$  can be computed by using the projections onto convex sets (POCS) algorithm: for  $i = 0, 2, 4, \dots$ ,  $\mathbf{P}^{i+1} = \Pi_{\mathcal{P}_1}(\mathbf{P}^i)$  with  $\Pi_{\mathcal{P}_1}(\mathbf{P}) = \left[ P_\ell \cdot 1_{\{P_\ell \leq \frac{\epsilon}{g_\ell}\}} + \frac{\epsilon}{g_\ell} \cdot 1_{\{P_\ell > \frac{\epsilon}{g_\ell}\}}, \quad \ell \in [L] \right]$ , and  $\mathbf{P}^{i+2} = \Pi_{\mathcal{P}_2}(\mathbf{P}^{i+1})$  with  $\Pi_{\mathcal{P}_2}(\mathbf{P}) = \mathbf{P} \cdot 1_{\{\sum_{\ell=1}^L P_\ell \leq P_0\}} + \frac{\mathbf{P} \cdot \sum_{\ell=1}^L P_\ell}{\sum_{\ell=1}^L P_\ell} \cdot 1_{\{\sum_{\ell=1}^L P_\ell > P_0\}}$ , where  $1_{\{\cdot\}}$  is an indicator. The penalty factor  $\eta$  in (12) follows a linear growth and is updated every  $N$  iterations of PGA. Specifically, at the  $n^{\text{th}}$  update step in (15),  $\mathcal{F}$  is given by  $\mathcal{F}(\mathbf{P}^{(n)}, \eta_n, b^{(n)})$ , where  $\eta_n$  is set as

$$\eta_n = \eta_0 \left( 1 + \gamma \left\lfloor \frac{n}{N} \right\rfloor \right), \quad (16)$$

where  $\gamma > 0$  is a constant that controls the growth rate. The PGA iteration in (15) stops when it reaches convergence, i.e.,

$$\max \left\{ \|\mathbf{P}^{(n)} - \mathbf{P}^{(n-1)}\|, |b^{(n)} - b^{(n-1)}| \right\} < \delta. \quad (17)$$

Upon convergence, if  $\Delta(\mathbf{P}) \geq 0$ ,  $\mathbf{P}^{(n)}$  is feasible and output as the solution to (3). Otherwise, the PGA does not find a feasible solution, and (6) is output as the solution to (3).

**Complexity Analysis:** Let the stopping rule for the bisection search of  $\zeta$  in (10) be  $\frac{|P_0 - \sum_{\ell=1}^L P_\ell^{\text{KKT}}(\zeta)|}{P_0} \leq \tau$ , and denote by  $T_\delta$  the number of PGA steps to meet the stopping rule in (17). The complexity of the feasibility check in (5) together with the trivial solution calculation in (6) is  $\mathcal{O}(L)$ . Next, for the convex power allocation, the bisection search takes  $\mathcal{O}(\log(1/\tau))$  iterations, and the complexity of computing the total power  $\sum_{\ell=1}^L P_\ell(\zeta)$  in each iteration is  $\mathcal{O}(L)$ , hence the overall complexity is  $\mathcal{O}(L \log(1/\tau))$ . Finally, for the PGA, since the computations in (11), (14), and (15) each has a complexity of  $\mathcal{O}(L)$ , the overall complexity is  $\mathcal{O}(LT_\delta)$ . Hence the overall complexity is  $\mathcal{O}(L(\log(1/\tau) + T_\delta))$ .

### B. Rate Allocation Under Non-causal CSI

Now we consider the rate allocation problem in (4) for minimum total power under non-causal CSI. Similar to Sec. III-A, the solution consists of three steps.

1) *Infeasibility check:* Unlike the rate maximization problem in (3), for the power minimization problem in (4), we only have the following two sufficient conditions for infeasibility. First, if condition (5) is not satisfied, then the covert rate is zero and therefore problem (4) is infeasible. Second, since  $P_\ell^{\max} = \frac{\epsilon}{g_\ell}$ , let  $R_\ell^{\max} = \log\left(1 + \frac{\epsilon h_\ell}{g_\ell}\right)$ ,  $\ell \in [L]$ . Then if

$$\sum_{\ell=1}^L R_\ell^{\max} < R_0, \quad (18)$$

the problem in (4) is also infeasible. If these two infeasibility conditions both do not hold, we drop the less noisy constraint in (4d) and solve the resulting convex rate allocation problem.

2) *Convex Rate Allocation:* Since (18) does not hold, by dropping the less noisy constraint in (4d),  $\mathbf{R}^{\max}$  is a feasible solution to the resulting convex problem. Then we form the Lagrangian

$$\begin{aligned} \mathcal{L}(\mathbf{R}, \lambda, \boldsymbol{\mu}) = & \sum_{\ell=1}^L \frac{e^{R_\ell} - 1}{h_\ell} - \lambda \left( \sum_{\ell=1}^L R_\ell - R_0 \right) \\ & + \sum_{\ell=1}^L \mu_\ell \left[ (e^{R_\ell} - 1) \frac{g_\ell}{h_\ell} - \epsilon \right], \end{aligned} \quad (19)$$

where  $\mathbf{R} = [R_1, \dots, R_L]$  and  $\boldsymbol{\mu} = [\mu_1, \dots, \mu_L]$ . Since  $R_\ell \geq 0$ ,  $\ell \in [L]$ , we write down the KKT conditions as follows:

$$\frac{\partial \mathcal{L}(\mathbf{R}, \lambda, \boldsymbol{\mu})}{\partial R_\ell} \geq 0 \Rightarrow R_\ell \geq \log\left(\frac{\lambda h_\ell}{1 + \mu_\ell g_\ell}\right), \quad \ell \in [L], \quad (20a)$$

$$\begin{aligned} \left( \frac{\partial \mathcal{L}(\mathbf{R}, \lambda, \boldsymbol{\mu})}{\partial R_\ell} \right) R_\ell &= 0 \\ \Rightarrow \left( (1 + \mu_\ell g_\ell) \frac{e^{R_\ell}}{h_\ell} - \lambda \right) R_\ell &= 0, \quad \ell \in [L], \end{aligned} \quad (20b)$$

$$\begin{aligned} \sum_{\ell=1}^L R_\ell - R_0 &\geq 0, \quad \lambda \geq 0, \quad \lambda \left( \sum_{\ell=1}^L R_\ell - R_0 \right) = 0, \quad (20c) \\ (e^{R_\ell} - 1) \frac{g_\ell}{h_\ell} - \epsilon &\leq 0, \quad \mu_\ell \geq 0, \end{aligned}$$

$$\mu_\ell \left[ (e^{R_\ell} - 1) \frac{g_\ell}{h_\ell} - \epsilon \right] = 0, \quad \ell \in [L]. \quad (20d)$$

If  $R_\ell = 0$ , from (20d)  $\mu_\ell = 0$ . Hence by (20a)  $\lambda \leq \frac{1}{h_\ell}$ . On the other hand, if  $R_\ell > 0$ , from (20b)  $R_\ell = \log\left(\frac{\lambda h_\ell}{1 + \mu_\ell g_\ell}\right)$ . Since  $\mu_\ell \geq 0$ ,  $\lambda h_\ell \geq \frac{\lambda h_\ell}{1 + \mu_\ell g_\ell} > 1$ . Therefore

$$R_\ell = \begin{cases} 0, & \lambda \leq \frac{1}{h_\ell}, \\ \log\left(\frac{\lambda h_\ell}{1 + \mu_\ell g_\ell}\right), & \lambda > \frac{1}{h_\ell}. \end{cases} \quad (21)$$

Furthermore, if  $\mu_\ell > 0$ , from (20d)  $R_\ell = \log\left(1 + \frac{\epsilon h_\ell}{g_\ell}\right)$ . And by (20b)  $R_\ell = \log\left(\frac{\lambda h_\ell}{1 + \mu_\ell g_\ell}\right) < \log(\lambda h_\ell)$ . Hence we have  $\lambda > \frac{1}{h_\ell} + \frac{\epsilon}{g_\ell}$ . On the other hand, if  $\mu_\ell = 0$ , by (20b)  $R_\ell = \log(\lambda h_\ell)$  and by (20d)  $R_\ell \leq \log\left(1 + \frac{\epsilon h_\ell}{g_\ell}\right)$ . Hence we have  $\lambda \leq \frac{1}{h_\ell} + \frac{\epsilon}{g_\ell}$ . Combining these with (21), we have

$$R_\ell^{\text{KKT}} = \begin{cases} 0, & 0 < \lambda \leq \frac{1}{h_\ell}, \\ \log(\lambda h_\ell), & \frac{1}{h_\ell} < \lambda \leq \frac{\epsilon}{g_\ell} + \frac{1}{h_\ell}, \\ \log\left(1 + \frac{\epsilon h_\ell}{g_\ell}\right), & \lambda > \frac{\epsilon}{g_\ell} + \frac{1}{h_\ell}. \end{cases} \quad (22)$$

Now by (20c), if  $\lambda = 0$ ,  $\sum_{\ell=1}^L R_\ell \geq R_0$ , and by (20b),  $R_\ell = 0$ ,  $\ell \in [L]$ . Then to meet the constraint we have  $R_0 = 0$  and the covert rate is 0. Otherwise if  $R_0 > 0$ ,  $\lambda > 0$  and  $\sum_{\ell=1}^L R_\ell = R_0$  should be satisfied.

Finally based on the above analysis, the convex rate allocation  $\mathbf{R}^{\text{KKT}}$  is given by (22), where  $\lambda > 0$  is chosen such that  $\sum_{\ell=1}^L R_\ell^{\text{KKT}} = R_0$ . If  $\mathbf{R}^{\text{KKT}}$  satisfies the less noisy constraint (4d), then it is the optimal solution to the original problem in (4). Otherwise, in the last step we apply the projected gradient descent method to the non-convex optimization problem in (4), starting from  $\mathbf{R}^{\text{KKT}}$ .

3) *Projected gradient descent:* Define

$$\Delta(\mathbf{R}) = \sum_{\ell=1}^L R_\ell - \sum_{\ell=1}^L \log\left(1 + (e^{R_\ell} - 1) \frac{g_\ell}{h_\ell}\right). \quad (23)$$

Then the less noisy constraint in (4d) becomes  $\Delta(\mathbf{R}) \geq 0$ .

Using the penalty method, we convert the convex constraint in (4d) to a penalty term to form the following penalized objective function to be minimized

$$\mathcal{G}(\mathbf{R}, \eta, b) = \sum_{\ell=1}^L \frac{e^{R_\ell} - 1}{h_\ell} + \eta \left[ \Delta(\mathbf{R}) - b \right]^2, \quad (24)$$

where  $\eta > 0$  is the penalty factor and  $b \geq 0$  is an auxiliary variable.

The constraints in (4b) and (4c) form a convex feasible set: define  $R_\ell^{\max} \triangleq \log\left(1 + \frac{\epsilon h_\ell}{g_\ell}\right)$ , we have

$$\mathcal{B} = \left\{ \mathbf{R} \mid 0 \leq R_\ell \leq R_\ell^{\max}, \ell \in [L], \sum_{\ell=1}^L R_\ell \geq R_0 \right\}. \quad (25)$$

We initialize as  $\mathbf{R}^{(0)} = \mathbf{R}^{\text{KKT}}$ ,  $\ell \in [L]$ ,  $b^{(0)} = 0$ , and

$$\eta_0 = \frac{C}{\Delta^2(\mathbf{R}^{(0)})} \sum_{\ell=1}^L \frac{e^{R_\ell} - 1}{h_\ell}, \quad (26)$$

where  $C \gg 1$  is a constant, so that the initial penalized objective is  $(1+C) \sum_{\ell=1}^L \frac{e^{R_\ell-1}}{h_\ell} \gg 0$ . To minimize (24), we run the following projected gradient descent (PGD) procedure: for  $n = 0, 1, \dots$ ,

$$\begin{aligned} \mathbf{R}^{(n+1)} &= \Pi_{\mathcal{B}} \left[ \mathbf{R}^{(n)} - \alpha_1 \nabla_{\mathbf{R}} \mathcal{G} \right] \Big|_{\mathbf{R}=\mathbf{R}^{(n)}}, \\ b^{(n+1)} &= \Pi_{\mathbb{R}^+} \left[ b^{(n)} - \alpha_2 \frac{\partial \mathcal{F}}{\partial b} \right] \Big|_{b=b^{(n)}}. \end{aligned} \quad (27)$$

For the projector  $\Pi_{\mathcal{B}}$ , note that  $\mathcal{B}$  is an intersection of two convex sets, i.e.,  $\mathcal{B} = \mathcal{B}_1 \cap \mathcal{B}_2$ , where  $\mathcal{B}_1 = \{\mathbf{R} \mid 0 \leq R_\ell \leq R_\ell^{\max}\}$  and  $\mathcal{B}_2 = \{\mathbf{R} \mid \sum_{\ell=1}^L R_\ell \geq R_0\}$ . Then  $\Pi_{\mathcal{B}}(\mathbf{R})$  can be computed by using the POCS algorithm: for  $i = 0, 2, 4, \dots$ ,  $\mathbf{R}^{i+1} = \Pi_{\mathcal{B}_1}(\mathbf{R}^i)$  with  $\Pi_{\mathcal{B}_1}(\mathbf{R}) = \left[ R_\ell \cdot 1_{\{R_\ell \leq R_\ell^{\max}\}} + R_\ell^{\max} \cdot 1_{\{R_\ell > R_\ell^{\max}\}}, \ell \in [L] \right]$ , and  $\mathbf{R}^{i+2} = \Pi_{\mathcal{B}_2}(\mathbf{R}^{i+1})$  with  $\Pi_{\mathcal{B}_2}(\mathbf{R}) = \mathbf{R} \cdot 1_{\{\sum_{\ell=1}^L R_\ell \geq R_0\}} + \mathbf{R} \frac{R_0}{\sum_{\ell=1}^L R_\ell} \cdot 1_{\{\sum_{\ell=1}^L R_\ell < R_0\}}$ . The penalty factor  $\eta_n$  is updated every  $N$  PGD steps according to (16). The PGD iteration in (27) stops when it reaches convergence, i.e.,

$$\max \left\{ \|\mathbf{R}^{(n)} - \mathbf{R}^{(n-1)}\|, |b^{(n)} - b^{(n-1)}| \right\} < \delta. \quad (28)$$

Upon convergence, if  $\Delta(\mathbf{R}^{(n)}) \geq 0$ , then  $\mathbf{R}^{(n)}$  is feasible and output as the solution to (4). Otherwise we consider the power allocation in (6) and denote it as  $\mathbf{P}(\alpha)$ . Denote  $R_\ell(\alpha) = \log(1 + P_\ell(\alpha)h_\ell)$  and  $R_{\text{sum}}(\alpha) = \sum_{\ell=1}^L R_\ell(\alpha)$ . If  $R_{\text{sum}}(1) \geq R_0$ , then  $\mathbf{R}(1) = [R_1(1), \dots, R_L(1)]$  is a feasible solution to the original problem in (4). Since  $R_{\text{sum}}(\alpha)$  monotonically increases with  $\alpha$ , and  $R_{\text{sum}}(0) = 0$ , using bisection search we can find a unique  $\alpha_0 \in [0, 1]$ , such that,

$$\mathbf{R}(\alpha_0) = [R_1(\alpha_0), \dots, R_L(\alpha_0)], \text{ s.t. } R_{\text{sum}}(\alpha_0) = R_0. \quad (29)$$

On the other hand, if  $R_{\text{sum}}(1) < R_0$ , we declare that (4) is infeasible. Note that for the last case of infeasibility declaration, the original non-convex problem in (4) may still be feasible, but the suboptimal PGD method cannot find a feasible solution.

**Complexity Analysis:** The complexity of the non-causal rate allocation scheme is the same as that of the non-causal power allocation scheme, except for the worst case in (29), where the PGD does not converge to a feasible solution and a bisection search with tolerance  $\tau_\alpha$  is needed to find an alternative solution. Under this condition, the complexity is  $\mathcal{O}(L(\log(1/\tau) + \log(1/\tau_\alpha) + T_\delta))$ .

#### IV. POWER AND RATE ALLOCATIONS WITH CAUSAL CSI

In this section, we treat the causal versions of the problems in (3) and (4), where at each block  $\ell \in [L]$ , the power  $P_\ell$  and rate  $R_\ell$ , respectively, are computed sequentially based on the causal channel state information  $\{(h_k, g_k), k \in [\ell]\}$ . We formulate the corresponding power allocation problem as a MDP and use a DRL method, in particular, the DDQN method, to solve it. The sequential rate allocation is not an MDP, but we show that it can be solved approximately using the trained DDQN for power allocation.

##### A. Power Allocation Under Causal CSI

**1) MDP formulation and Q-learning:** Since the power allocation  $P_\ell$  is sequentially computed for each  $\ell \in [L]$ , the less noisy constraint in (3d) is enforced for each  $\ell$ :

$$\sum_{k=1}^{\ell} \log(1 + P_k h_k) \geq \sum_{k=1}^{\ell} \log(1 + P_k g_k), \ell \in [L]. \quad (30)$$

We next formulate the sequential power allocation to maximize the sum covert rate in (3a), subject to the constraints in (3b), (3c) and (30) as an MDP. Denote  $P^{(\ell)}$  as the remaining power before allocating power to the  $\ell^{\text{th}}$  block, and  $P_\ell$  as the power allocated to the  $\ell^{\text{th}}$  block. Then we have

$$P^{(1)} = P_0, \quad P^{(\ell+1)} = P^{(\ell)} - P_\ell, \quad \ell \in [L-1]. \quad (31)$$

Moreover, define

$$\Gamma^{(1)} \triangleq 0, \quad \Gamma^{(\ell+1)} \triangleq \Gamma^{(\ell)} + \log \left( \frac{1 + P_\ell h_\ell}{1 + P_\ell g_\ell} \right), \quad \ell \in [L-1]. \quad (32)$$

Then the constraints in (30) become

$$\Gamma^{(\ell)} \geq 0, \quad \ell \in [L]. \quad (33)$$

In our MDP formulation, for each  $\ell \in [L]$ , the state is defined as  $\mathbf{s}_\ell = (P^{(\ell)}, \Gamma^{(\ell)}, h_\ell, g_\ell)$ , and the action is  $P_\ell$ . Recall that the channel SNRs  $h_\ell$  and  $g_\ell$  are quantized, and similarly we assume that the power allocation  $P_\ell \in \mathcal{P} = \{n\Delta_P, n = 0, 1, 2, \dots\}$  where  $\Delta_P$  is the quantization step size. Based on (3b), (31) and (3c), we have  $0 \leq P_\ell \leq P^{(\ell)}$  and  $0 \leq P_\ell \leq \frac{C}{g_\ell}$ . Furthermore, to meet the constraints in (33), we have

$$\begin{aligned} \Gamma^{(\ell+1)} &= \Gamma^{(\ell)} + \log \left( \frac{1 + h_\ell P_\ell}{1 + g_\ell P_\ell} \right) \geq 0 \\ \Leftrightarrow P_\ell \left( e^{-\Gamma^{(\ell)}} g_\ell - h_\ell \right) &\leq 1 - e^{-\Gamma^{(\ell)}}. \end{aligned} \quad (34)$$

Hence the feasible set of the action  $P_\ell$  is given by (35). At each block  $\ell$ , an action  $P_\ell \in \mathcal{A}_\ell$  is selected based on the current state  $\mathbf{s}_\ell$ , according to a policy  $\pi(P|\mathbf{s}) = \mathbb{P}(P_\ell = P|\mathbf{s}_\ell = \mathbf{s})$ , which defines the probability distribution over actions given the state. The state then transitions to a new one  $\mathbf{s}_{\ell+1}$ , yielding a reward  $r_{\ell+1}$ , which is the covert rate, given by

$$r_{\ell+1} = r(\mathbf{s}_\ell, P_\ell) \triangleq \log(1 + h_\ell P_\ell). \quad (36)$$

These variables together form an MDP experience, denoted as  $\mathbf{e} = (\ell, \mathbf{s}_\ell, P_\ell, \mathbf{s}_{\ell+1}, r_{\ell+1})$ . Assuming that  $L$  is large, for a given policy  $\pi$ , the expected cumulative reward function at each block, commonly known as the Q-function, is defined as

$$\begin{aligned} Q_\pi(\mathbf{s}, P) &= r(\mathbf{s}, P) \\ &+ \mathbb{E}_{P_k \sim \pi(\cdot|\mathbf{s}_k)} \left[ \sum_{k=\ell+1}^L r(\mathbf{s}_k, P_k) \mid \mathbf{s}_\ell = \mathbf{s}, P_\ell = P \right]. \end{aligned} \quad (37)$$

The optimal policy  $\pi^*$  satisfies  $Q_{\pi^*}(\mathbf{s}, P) \geq Q_\pi(\mathbf{s}, P)$  for all state-action pairs  $(\mathbf{s}, P)$  and all other policies  $\pi$ . Note that any finite MDP admits an optimal deterministic policy [28, Theorem 17.8].

A basic method to find the optimal policy  $\pi^*$  is Q-learning, an iterative algorithm that learns from episodes of experiences.

$$\mathcal{A}_\ell = \left\{ P \in \mathcal{P} \mid P \leq \min \left\{ P^{(\ell)}, \frac{\epsilon}{g_\ell} \right\}, \text{ if } e^{-\Gamma^{(\ell)}} g_\ell \leq h_\ell \text{ \& } P \leq \min \left\{ P^{(\ell)}, \frac{\epsilon}{g_\ell}, \frac{1 - e^{-\Gamma^{(\ell)}}}{e^{-\Gamma^{(\ell)}} g_\ell - h_\ell} \right\}, \text{ otherwise} \right\} \quad (35)$$

Suppose that the  $j^{\text{th}}$  experience corresponds to block  $\ell$ . Then given the state  $\mathbf{s}_\ell$ , the  $\xi$ -greedy policy is applied using the current Q-function to select the action  $P_\ell$ : it takes the greedy action  $P_\ell = \arg\max_{P \in \mathcal{A}_\ell} Q(\mathbf{s}_\ell, P)$  with probability  $(1 - \xi)$  or randomly chooses an action  $P_\ell \in \mathcal{A}_\ell$  with probability  $\xi$ . Then the reward  $r_{\ell+1}$  in (36) is obtained and the state transitions to  $\mathbf{s}_{\ell+1}$ . The  $j^{\text{th}}$  experience  $e_j = (\ell, \mathbf{s}_\ell, P_\ell, \mathbf{s}_{\ell+1}, r_{\ell+1})$  is used to update the entry  $(\mathbf{s}_\ell, P_\ell)$  of the Q-function, as follows,

$$Q(\mathbf{s}_\ell, P_\ell) \leftarrow (1 - \beta)Q(\mathbf{s}_\ell, P_\ell) + \beta \left( r_{\ell+1} + \max_{P_{\ell+1} \in \mathcal{A}_{\ell+1}} Q(\mathbf{s}_{\ell+1}, P_{\ell+1}) \right), \quad (38)$$

where  $\beta \in (0, 1]$  is a learning rate parameter. However, in this case, the cardinality of the state space, i.e., the total number of possible values that the state  $\mathbf{s}_\ell$  can take, is very large. Therefore it is impractical to obtain the Q-function values for all state-action pairs, and we resort to the neural network representation of the Q-function, i.e., the deep Q-learning network (DQN).

2) *DDQN solution*: The double deep Q-learning network (DDQN) consists of a primary Q-network  $Q(\mathbf{s}, P; \Theta)$  and a target Q-network  $\hat{Q}(\mathbf{s}, P; \hat{\Theta})$ , with the input to each Q-network as the state-action pair  $(\mathbf{s}, P)$ , and the output as the corresponding Q-function value. The primary Q-network is periodically copied into the target Q-network every  $N_{\text{ep}}$  training episodes to ensure more stable updates (line 23 of Alg. 1). At each training episode,  $N_{\text{tr}}$   $L$ -state transitions are carried out based on the current primary network  $Q(\mathbf{s}, P; \Theta)$ , and the corresponding experiences are stored in the replay buffer  $\mathcal{D}$  of size  $N_{\text{buff}}$  (lines 6-18 of Alg. 1). Specifically, similar to the conventional Q-learning algorithm, each training experience  $e_\ell = (\ell, \mathbf{s}_\ell, P_\ell, \mathbf{s}_{\ell+1}, r_{\ell+1})$  is generated based on the  $\xi$ -greedy policy: given the current state  $\mathbf{s}_\ell$ , the policy selects the greedy action  $P_\ell = \arg\max_{P \in \mathcal{A}_\ell} Q(\mathbf{s}_\ell, P; \Theta)$  with probability  $(1 - \xi)$  or randomly chooses an action  $P_\ell \in \mathcal{A}_\ell$  with probability  $\xi$ . To balance the exploration-exploitation,  $\xi$  is initialized as  $\xi_{\text{max}}$  and decreases linearly at each episode until it reaches the lower bound  $\xi_{\text{min}}$ , which is then maintained until the end of training (line 22 of Alg. 1).

After updating the replay buffer  $\mathcal{D}$ , a random batch of experiences  $\{\tilde{e}_1, \dots, \tilde{e}_{N_b}\}$  is sampled from  $\mathcal{D}$  to update the primary Q-network, using the stochastic gradient descent (SGD) (lines 19-21 of Alg. 1). In particular, for a given experience  $\tilde{e}_j = (\ell, \mathbf{s}_\ell, P_\ell, \mathbf{s}_{\ell+1}, r_{\ell+1})$ , the corresponding loss is defined as: first define the target Q-value of DDQN as

$$Y(\tilde{e}_j) = r_{\ell+1} + \hat{Q}(\mathbf{s}_{\ell+1}, \arg\max_{P \in \mathcal{A}_{\ell+1}} Q(\mathbf{s}_{\ell+1}, P; \Theta); \hat{\Theta}). \quad (39)$$

Based on the Q-learning update in (38), the loss associated with  $\tilde{e}_j$  is then given by the mean-squared error between the

target Q-value in (39) and the predicted Q-value  $Q(\mathbf{s}_\ell, P_\ell; \Theta)$ , i.e.,

$$L_\Theta(\tilde{e}_j) = [Y(\tilde{e}_j) - Q(\mathbf{s}_\ell, P_\ell; \Theta)]^2. \quad (40)$$

When  $\ell = L$ , we set  $Q(\mathbf{s}_{L+1}, P_{L+1}; \Theta) = \hat{Q}(\mathbf{s}_{L+1}, P_{L+1}; \hat{\Theta}) = 0$ . With the loss given by (40) and (39), the primary network parameter is then updated using the SGD, as

$$\Theta \leftarrow \Theta - \gamma \cdot \nabla_\Theta \left( \sum_{j=1}^{N_b} L_\Theta(\tilde{e}_j) \right). \quad (41)$$

The pseudo-code for DDQN training is summarized in Algorithm 1. Given a trained primary Q-network  $Q(\mathbf{s}, P; \Theta^*)$ , the causal power allocation is then given by

$$P_\ell = \arg\max_{P \in \mathcal{A}_\ell} Q(\mathbf{s}_\ell, P; \Theta^*), \quad \ell \in [L]. \quad (42)$$

### B. Rate Allocation Under Causal CSI

Unlike the causal power allocation scheme in Sec. IV-A, the rate allocation under causal CSI cannot be formulated as an MDP due to the total rate constraint in (4b). Specifically, for power allocation, by defining the state variable  $P^{(\ell)}$  in (31), the total power constraint in (3b) can be written as  $P_\ell \leq P^{(\ell)}$ , i.e., the current action is constrained by the current state. On the other hand, for rate allocation, the action variable is  $R_\ell$  and if we similarly define the state variable

$$R^{(1)} = R_0, \quad R^{(\ell+1)} = R^{(\ell)} - R_\ell, \quad \ell \in [L-1]. \quad (43)$$

Then the total rate constraint becomes  $\sum_{j=\ell}^L R_j \geq R^{(\ell)}$ , i.e., the future actions are constrained by the current state. Hence the rate allocation is non-Markovian and therefore cannot be formulated as an MDP.

Here we employ a trained power allocation network  $Q(\mathbf{s}, P; \Theta^*)$  in (42) to approximately solve the causal rate allocation problem. Note that  $R_\ell \triangleq \log(1 + h_\ell P_\ell)$ , hence we denote  $\mathcal{R}(x) \triangleq \log(1 + x)$  and  $\mathcal{R}^{-1}(x) \triangleq 2^x - 1$ . We have

$$\begin{aligned} R^{(\ell)} &\leq \sum_{i=\ell}^L R_i = \sum_{i=\ell}^L \mathcal{R}(h_i P_i) \\ &\leq (L - \ell + 1) \cdot \mathcal{R} \left( \frac{\sum_{i=\ell}^L h_i P_i}{L - \ell + 1} \right), \end{aligned} \quad (44)$$

where the first inequality is due to (4b), and the second inequality follows from Jensen's inequality. Hence

$$\sum_{i=\ell}^L h_i P_i \geq (L - \ell + 1) \cdot \mathcal{R}^{-1} \left( \frac{R^{(\ell)}}{L - \ell + 1} \right). \quad (45)$$

Denote  $\bar{h} \triangleq \mathbb{E}(h)$  as the expected legitimate channel SNR. Then we approximate the left-hand side of (45) by

---

**Algorithm 1** DDQN training for causal power allocation.

---

- 1: **Channel parameters:** total power  $P_0$ , number of coherent blocks  $L$ , legitimate receiver SNR $_H$ , warden SNR $_G$ , covert constraint  $\epsilon$
  - 2: **Algorithm hyperparameters:** replay buffer size  $N_{\text{buff}}$ , number of  $L$ -state transitions  $N_{\text{tr}}$ , number of episodes per target Q-network update  $N_{\text{ep}}$ , batch size of experiences  $N_b$ ,  $\epsilon$ -greedy parameters  $(\xi_{\min}, \xi_{\max}, \delta_\xi)$ , learning rate  $\gamma$
  - 3: Initialize the replay experience buffer  $\mathcal{D}$ ,  $\xi = \xi_{\max}$
  - 4: Randomly initialize network parameters  $\Theta$  and  $\hat{\Theta}$
  - 5: **for** episode  $E = 0, 1, 2, \dots$  **do**
  - 6:   **for** state transition  $n = 1, \dots, N_{\text{tr}}$  **do**
  - 7:     Randomly generate  $\{h_\ell\}_{\ell=1}^L$  and  $\{g_\ell\}_{\ell=1}^L$ , let  $P^{(1)} = P_0$ ,  $\Gamma^{(1)} = 0$
  - 8:     **for**  $\ell = 1, \dots, L$  **do**
  - 9:       Generate the action  $P_\ell$  based on  $\xi$ -greedy policy
  - 10:       **if**  $\ell = L$  **then**
  - 11:           $P^{(L+1)} = 0$ ,  $\Gamma^{(L+1)} = 0$  and  $s_{L+1} = 0$
  - 12:       **else**
  - 13:          Compute  $P^{(\ell+1)}$ ,  $\Gamma^{(\ell+1)}$  and  $r_{\ell+1}$  based on (31), (32) and (36), respectively.
  - 14:          **If**  $|\mathcal{D}| \geq N_{\text{buff}}$ , pop out the oldest experience
  - 15:          Add  $e_\ell = (\ell, s_\ell, P_\ell, s_{\ell+1}, r_{\ell+1})$  to  $\mathcal{D}$
  - 16:       **end if**
  - 17:     **end for**
  - 18:   **end for**
  - 19:   Randomly select  $N_b$  experiences  $\{\tilde{e}_j\}_{j=1}^{N_b}$  from  $\mathcal{D}$
  - 20:   Compute the losses  $\{L_\Theta(\tilde{e}_j)\}_{j=1}^{N_b}$  using (40) and (39)
  - 21:   Update  $\Theta$  by SGD using (41)
  - 22:    $\xi = \max\{\xi_{\min}, \xi_{\max} - \delta_\xi \cdot E\}$
  - 23:    $\hat{\Theta} \leftarrow \Theta$  if  $E = 0 \bmod N_{\text{ep}}$
  - 24: **end for**
  - 25: **return** primary Q-network parameter  $\Theta^*$
- 

$\sum_{i=\ell}^L h_i P_i \approx P^{(\ell)} \cdot \bar{h}$ , where  $P^{(\ell)}$  is defined in (31). Therefore we can convert  $R^{(\ell)}$  to  $P^{(\ell)}$  as

$$P^{(\ell)}(R^{(\ell)}) = \frac{L - \ell + 1}{\bar{h}} \cdot \mathcal{R}^{-1} \left( \frac{R^{(\ell)}}{L - \ell + 1} \right). \quad (46)$$

In particular, we set  $P_0 = P^{(1)}(R^{(1)}) = \frac{L}{\bar{h}} \cdot \mathcal{R}^{-1}(\frac{R_0}{L})$  and train a primary Q-network  $Q(s, P; \Theta^*)$  using Algorithm 1. Then we use the trained network to compute the causal rate allocations  $R_\ell$  as follows. Starting from  $R^{(1)} = R_0$ ,  $\Gamma^{(1)} = 0$ , for each block  $\ell \in [L - 1]$ , given  $(R^{(\ell)}, \Gamma^{(\ell)}, h_\ell, g_\ell)$ , we first compute  $P^{(\ell)}(R^{(\ell)})$  in (46), and the feasible set of power allocation  $\mathcal{A}_\ell$  in (35), and select the power allocation  $P_\ell$  using the trained network  $Q(s, P; \Theta^*)$ :

$$P_\ell = \operatorname{argmax}_{P \in \mathcal{A}_\ell} Q(s_\ell, P; \Theta), \quad s_\ell = (P^{(\ell)}(R^{(\ell)}), \Gamma^{(\ell)}, h_\ell, g_\ell). \quad (47)$$

Next, we compute  $R_\ell(P_\ell) = \log(1 + h_\ell P_\ell)$  and update

$$R^{(\ell+1)} = R^{(\ell)} - R_\ell(P_\ell), \quad \Gamma^{(\ell+1)} = \Gamma^{(\ell)} + \log \left( \frac{1 + h_\ell P_\ell}{1 + g_\ell P_\ell} \right). \quad (48)$$

For the last block  $L$ , given  $(R^{(L)}, \Gamma^{(L)}, h_L, g_L)$  and  $P^{(L)}(R^{(L)}) = \frac{e^{R^{(L)}} - 1}{h_L}$ , we compute the feasible set  $\mathcal{A}_L$  using (35) and declare infeasibility if  $\max_{P_L \in \mathcal{A}_L} \log(1 + h_L P_L) < R^{(L)}$ ; otherwise we set  $R_L = R^{(L)}$  and the above sequential rate allocation provides a feasible solution.

## V. SIMULATION RESULTS

### A. Simulation Setup

1) *Quantized Channels:* The legitimate receiver's and the warden's channels in (1) are generated as  $H_\ell \sim \mathcal{CN}(0, \sigma_H^2)$  and  $G_\ell \sim \mathcal{CN}(0, \sigma_G^2)$ . The instantaneous SNRs  $h_\ell = \frac{|H_\ell|^2}{\sigma_n^2}$  and  $g_\ell = \frac{|G_\ell|^2}{\sigma_v^2}$  are quantized into 1024 levels. The average SNR of these two channels are defined as

$$\text{SNR}_H \triangleq 10 \log_{10} \left( \frac{\sigma_H^2}{\sigma_n^2} \right), \quad \text{SNR}_G \triangleq 10 \log_{10} \left( \frac{\sigma_G^2}{\sigma_v^2} \right). \quad (49)$$

We set the block size  $L = 10$ .

2) *Baseline Methods:* We consider two baseline methods for solving the non-causal power allocation optimization problem in (3) if it is feasible: the first method, referred to as "trivial", is given by (6), and the second method, referred to as "convex", is given by the solution to the convex problem (3a)-(3c) if this convex solution satisfies (3d), and otherwise it is given by (6). We also consider two baseline methods for solving the non-causal rate allocation optimization problem in (4) if the infeasibility conditions in (5) and (18) both do not hold: the first one, referred to as "trivial", is given by (29) if it satisfies (4d), otherwise it declares infeasibility; and the second one, referred to as "convex", is given by (22) if this convex solution satisfies (4d), and otherwise it is given by the trivial baseline.

Also, two baseline methods are considered for solving the sequential power allocation problem under causal CSI. The first method termed "average" is proposed in [29], which assigns the current power  $P_\ell$  to maximize the total future rate by setting the legitimate channel SNR as the expected value, i.e.,  $h_j = \bar{h} \triangleq \mathbb{E}(h)$ , and the remaining power is evenly split, i.e.,  $P_j = \frac{P^{(\ell)} - P_\ell}{L - \ell}$ , for  $j = \ell + 1, \dots, L$ . That is,

$$\hat{P}_\ell = \operatorname{argmax}_{P \in \mathcal{A}_\ell} \left\{ \log(1 + P h_\ell) + (L - \ell) \cdot \left[ \log \left( 1 + \frac{P^{(\ell)} - P}{L - \ell} \cdot \bar{h} \right) \right] \right\}. \quad (50)$$

When  $\ell = L$ ,  $\hat{P}_L = \max\{P \in \mathcal{A}_L\}$ . The other baseline, referred to as "trivial", is the causal version of the trivial non-causal baseline in (6): for each block  $\ell$ ,  $P_\ell = 0$  if  $h_\ell < g_\ell$  and  $P_\ell = \frac{\epsilon}{g_\ell}$  otherwise, until reaching the total power constraint  $P_0$ . We also consider two baseline methods for the causal rate allocation problem. One termed "average" operates as follows [29]: given the remaining rate  $R^{(\ell)}$  and the auxiliary variable  $\Gamma^{(\ell)}$  for each block  $\ell \in [L - 1]$ , it computes  $P^{(\ell)}(R^{(\ell)})$  using (46) and  $\hat{P}_\ell$  using (50), then it computes  $R_\ell(\hat{P}_\ell) = \log(1 + h_\ell \hat{P}_\ell)$  and updates  $R^{(\ell+1)}$  and  $\Gamma^{(\ell+1)}$  by (48). When  $\ell = L$ , it declares infeasibility if  $\max_{P \in \mathcal{A}_L} \log(1 + h_L P) < R^{(L)}$ ; otherwise it sets  $R_L =$



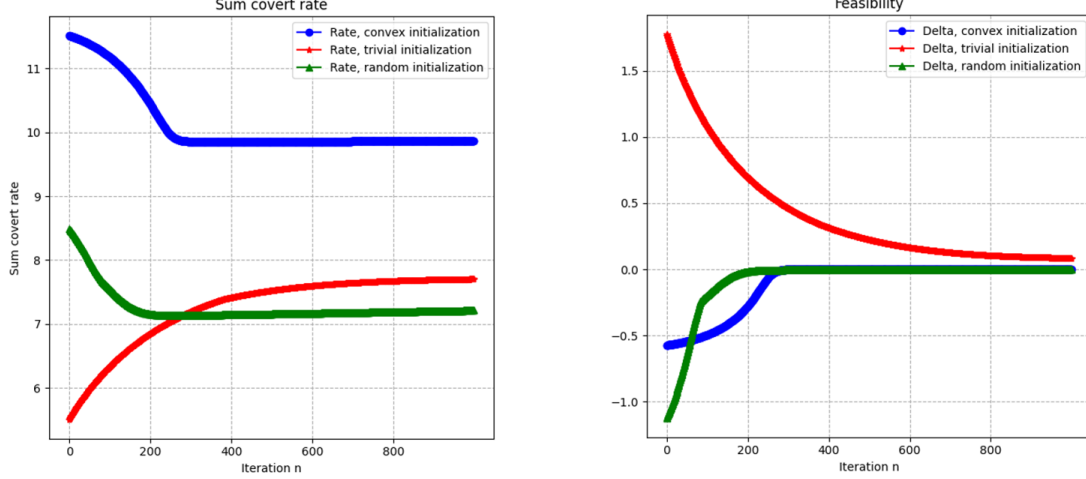


Fig. 2: Convergence of the projected gradient ascent procedure in Sec. III-A3 for rate maximization, with different initializations.

$R^{(L)}$  and obtains a feasible solution. The other baseline termed “trivial” operates as follows: for each block  $\ell$ , it assigns  $R_\ell = 0$  if  $h_\ell < g_\ell$  and  $R_\ell = \log\left(1 + \frac{\epsilon h_\ell}{g_\ell}\right)$  otherwise, until reaching the total rate requirement  $R_0$ ; if  $R_0$  cannot be achieved, it declares infeasibility.

#### B. Power Allocation Under Non-causal CSI

We now illustrate the performance of our proposed algorithm in Sec. III-A for solving the power allocation problem in (3). We first show the convergence of the PGA procedure in Sec. III-A3. Recall that it is initialized as the convex solution in (10) which is an infeasible upper bound on the sum covert rate, i.e.,  $\Delta(\mathbf{P}) < 0$ . We set  $\text{SNR}_H = 5\text{dB}$ ,  $\text{SNR}_G = 5\text{dB}$  in (49),  $P_0 = 5\text{dB}$  in (3b),  $\epsilon = 0\text{dB}$  in (3c),  $C = 20$  in (14),  $\alpha_1 = \alpha_2 = 10^{-6}$  in (15),  $N = 10$  and  $\gamma = 0.2$  in (16) and  $\delta = 10^{-6}$  in (17). In Fig. 2 we plot the sum covert rate and  $\Delta(\mathbf{P})$  over the iteration  $n$ , for a fixed realization of  $(H_\ell, G_\ell)$ ,  $\ell \in [L]$ . It is seen that the PGA steadily increases  $\Delta(\mathbf{P})$  and forces it to approach zero, while the sum covert rate converges to a lower value than the convex solution in (10) to meet the less noisy constraint. As a comparison, in the same figure, we also show the convergence when initialized with the trivial solution in (6), which is feasible, i.e.,  $\Delta(\mathbf{P}) > 0$ , but with a very low sum covert rate. It is seen that in this case  $\Delta(\mathbf{P})$  decreases to zero over the iteration, but the sum covert rate converges to a much lower value. Furthermore, the convergence with a random initialization is shown in Fig. 2. Our simulations show that with random initialization, the converged sum covert rate can be either lower or higher than that with the trivial initialization, but it is always lower than that with the convex initialization. Hence Fig. 2 demonstrates the importance of initialization to the quality of the converged solution of the PGA procedure, and the infeasible convex solution in (10) serves as an effective initialization.

Next, in Fig. 3 we plot the average sum covert rate versus the total power constraint  $P_0$  by the proposed method, the “convex” baseline method, and the “trivial” baseline method.

The results indicate that the proposed scheme consistently outperforms the baseline schemes, while the convex baseline achieves a higher covert rate than the trivial baseline. Furthermore, the advantage of the proposed scheme becomes more pronounced when the warden has a better channel and when the total power constraint  $P_0$  is higher. Additionally, a smaller  $\epsilon$  results in a lower covert rate due to the stricter covertness constraint.

#### C. Rate Allocation Under Non-causal CSI

In this section, we illustrate the performance of the proposed algorithm in Sec. III-B for solving the rate allocation problem in (4). We first show the convergence of the PGD procedure in Sec. III-B3. Recall that the convex initialization in (22) is an infeasible lower bound on the total power consumption, i.e.,  $\Delta(\mathbf{R}) < 0$ . We set  $\text{SNR}_H = 5\text{dB}$ ,  $\text{SNR}_G = 5\text{dB}$ ,  $R_0 = 5$  in (4b),  $\epsilon = 0\text{dB}$  in (4c),  $C = 20$  in (26),  $\alpha_1 = \alpha_2 = 10^{-6}$  in (27),  $N = 10$  and  $\gamma = 0.2$  in (16) and  $\delta = 10^{-6}$  in (28). Fig. 4 shows the total power consumption and  $\Delta(\mathbf{R})$  over the iteration  $n$ , for a fixed realization of  $(H_\ell, G_\ell)$ ,  $\ell \in [L]$ . It is seen that the PGD steadily increases  $\Delta(\mathbf{R})$  and forces it to approach zero, while the power consumption converges to a higher value than the convex solution in (22) to meet the less noisy constraint. For comparison, in the same figure we plot the convergence when initialized with the trivial solution in (29), which may or may not be feasible, and the convergence with a random initialization. It is seen that both initializations result in converged power consumptions that are higher than that with the convex initialization.

In Fig. 5 we plot the feasibility probabilities of different schemes under two covertness constraints  $\epsilon = 0\text{dB}$  and  $\epsilon = -5\text{dB}$ . As before, we consider two SNR scenarios: (a)  $\text{SNR}_H = \text{SNR}_G = 5\text{dB}$ , and (b)  $\text{SNR}_H = 5\text{dB}$ ,  $\text{SNR}_G = 10\text{dB}$ . It is observed that the feasibility probabilities become lower when the required sum rate  $R_0$  increases. Comparing Fig. 5a and Fig. 5b, we find that when the warden channel is better than the legitimate channel, the feasibility probabilities

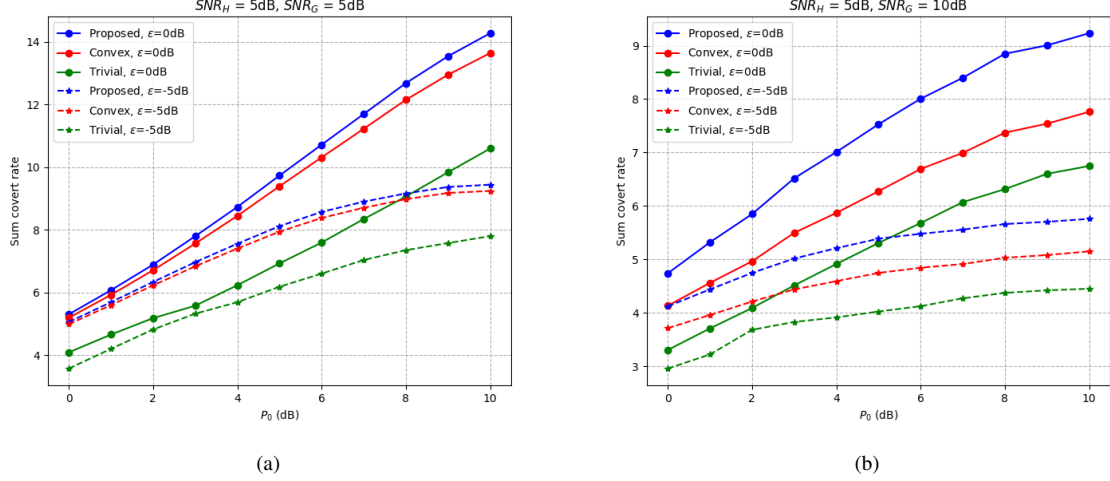


Fig. 3: Sum covert rates under non-causal power allocation schemes.

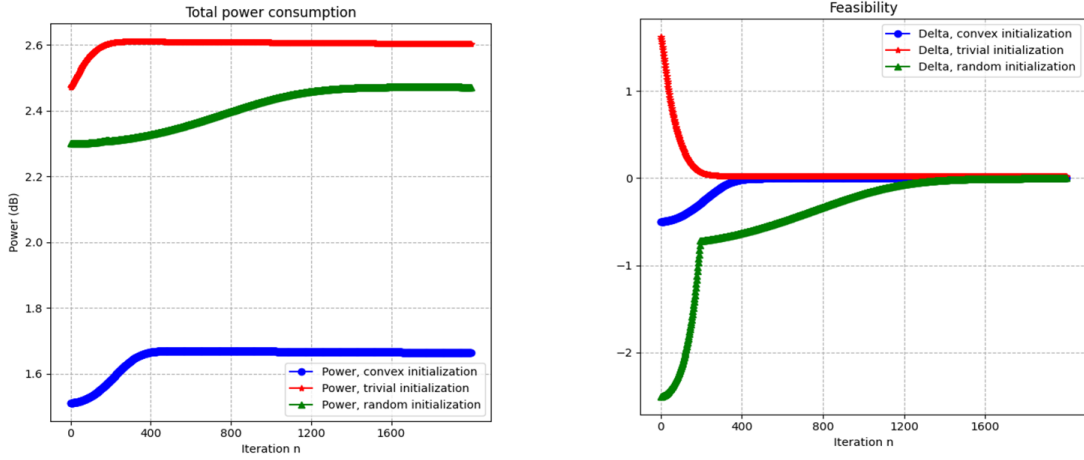


Fig. 4: Convergence of the projected gradient descent procedure in Sec. III-B3 for power minimization, with different initializations.

decrease substantially for all three schemes. However, for both scenarios, the proposed scheme has a significantly higher feasibility probability than the “convex” and the “trivial” baselines. Furthermore, a smaller  $\epsilon$  reduces the feasibility probabilities, since meeting the sum rate constraint in (4b) becomes more challenging under a stricter covertness constraint.

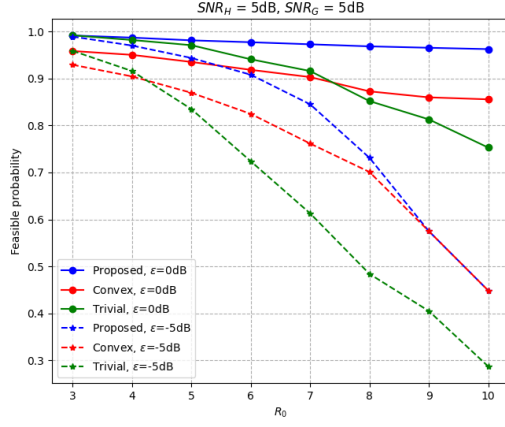
Next, in Fig. 6 we compare the average power consumptions when the proposed scheme and the two baselines all output feasible solutions. It is seen that the proposed scheme consistently achieves a lower power consumption than the two baselines, while the convex baseline consumes less power than the trivial baseline. Note that the actual sum rates achieved by the baseline schemes match the required rate  $R_0$ , since both the convex solution (22) and the trivial solution (29) satisfy  $R_{\text{sum}} = R_0$ ; whereas the proposed scheme achieves a sum rate exceeding  $R_0$ , as the PGD typically converges to a feasible rate allocation with  $R_{\text{sum}} > R_0$ .

#### D. Power Allocation Under Causal CSI

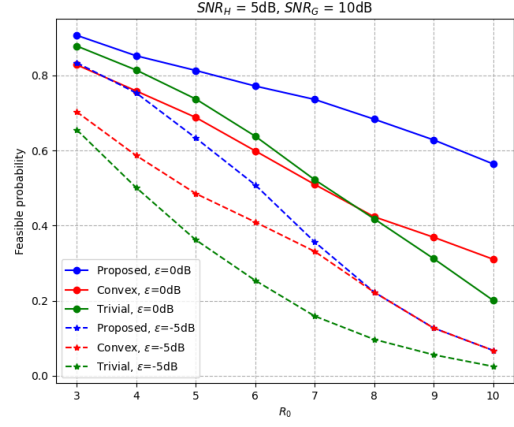
Now we illustrate the performance of our proposed DRL algorithm in Sec. IV-A for solving the sequential power

allocation problem under causal CSI. We first demonstrate the convergence of Algorithm 1 for DDQN training. The parameters are set as follows:  $P_0 = 5\text{dB}$ ,  $L = 10$ ,  $\epsilon = 0\text{dB}$ ,  $N_{\text{buff}} = 5 \times 10^3$ ,  $N_{\text{tr}} = 50$ ,  $N_{\text{ep}} = 5$ ,  $N_b = 64$ ,  $\xi_{\min} = 0.1$ ,  $\xi_{\max} = 1$ ,  $\delta_\xi = 10^{-4}$  and  $\gamma = 10^{-3}$ . In Fig. 7 we plot the convergence curves of the MSE loss and the sum covert rate over training episodes. Two SNR scenarios are considered: (a)  $SNR_H = SNR_G = 5\text{dB}$ , and (b)  $SNR_H = 5\text{dB}$ ,  $SNR_G = 10\text{dB}$ . The results indicate that as training progresses, the MSE loss gradually decreases while the sum covert rate increases. Furthermore, a favorable channel condition, i.e.,  $SNR_H = SNR_G = 5\text{dB}$ , leads to a higher sum covert rate and a lower MSE loss.

Next, in Fig. 8 we plot the average sum covert rate versus the total power constraint  $P_0$  of our proposed DDQN causal power allocation and compare it with the “average” and the “trivial” baseline methods, as well as the proposed non-causal method in Sec. III-A. It is observed that the DDQN power allocation scheme consistently outperforms the two baseline schemes, and the performance gain becomes more pronounced

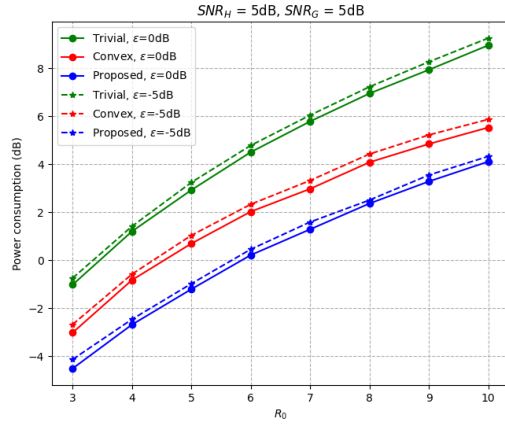


(a)

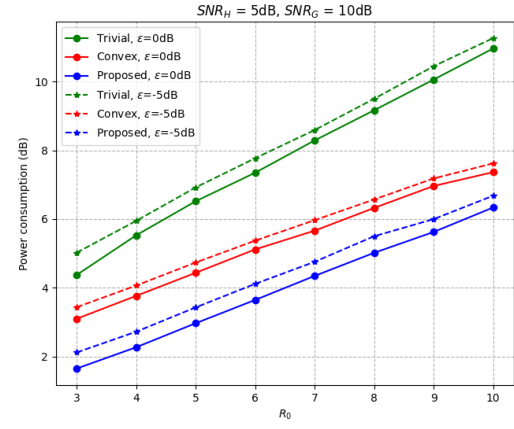


(b)

Fig. 5: Feasibility probabilities of non-causal rate allocation schemes.

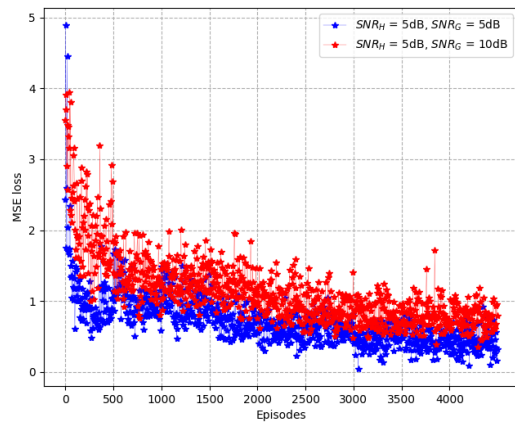


(a)

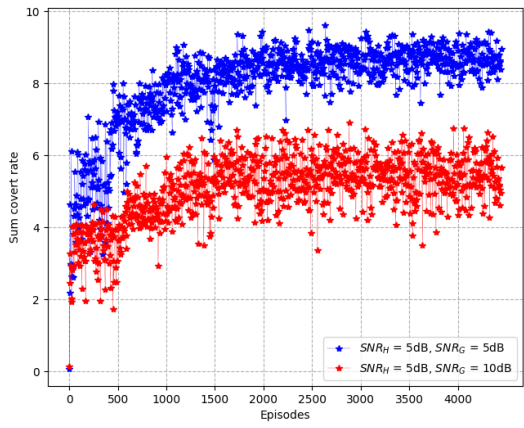


(b)

Fig. 6: Power consumptions under non-causal rate allocation schemes when they are all feasible.



(a)



(b)

Fig. 7: Convergence of Algorithm 1: MSE loss and sum covert rate versus training episodes.

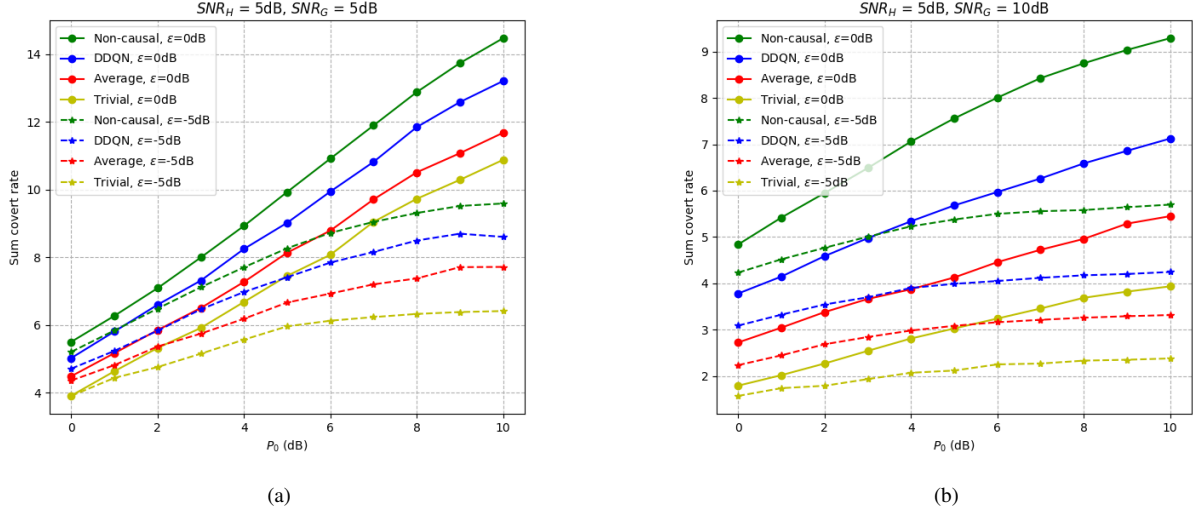


Fig. 8: Sum covert rates under causal power allocation schemes.

when the warden has a better channel. On the other hand, compared with the non-causal power allocation, there is a covert rate loss due to the causality of the CSI, which also increases when the warden's channel is better. Additionally, in both non-causal and causal cases, a smaller  $\epsilon$  results in a lower covert rate corresponding to a stricter covertness constraint.

#### E. Rate Allocation Under Causal CSI

Finally we demonstrate the performance of the proposed approximate DRL algorithm in Sec. IV-B for solving the sequential rate allocation problem under causal CSI. Fig. 9 shows the feasibility probabilities of the proposed DDQN-based rate allocation method, the "average" and the "trivial" baseline methods, and the proposed non-causal method in Sec. III-B. Fig. 10 shows the average power consumption versus the total required rate  $R_0$  for the same rate allocation schemes, under the condition that all schemes yield feasible solutions. It is observed from Fig. 10 and Fig. 9 that the DDQN rate allocation scheme consistently outperforms two baseline methods, in terms of achieving both lower total power consumption and higher feasibility probability. On the other hand, the gaps to the corresponding non-causal rate allocation become larger when the warden's channel is better. Moreover, in both non-causal and causal cases, a smaller  $\epsilon$  results in a higher power consumption and lower feasibility probability.

#### VI. CONCLUSIONS

We have developed transmission strategies to achieve keyless positive-rate covert communication in block-fading channels. Based on the results developed for DMCs, we first formulate power allocation and rate allocation as non-convex optimization problems. When the CSI of each fading block is known non-causally at the transmitter and legitimate receiver, we propose three-step methods to solve the corresponding power and rate optimization problems. For the case of causal CSI, the corresponding power allocation problem is formulated as an MDP and solved using a DDQN method. Although the

rate allocation problem under causal CSI is not an MDP, we solve it approximately using the DDQN trained for power allocation. Extensive simulation results are provided to demonstrate the high performance of the proposed power and rate allocation algorithms to achieve keyless positive-rate covert communications, under both non-causal and causal CSI.

#### REFERENCES

- [1] M. R. Bloch and J. Barros, *Physical-Layer Security: From Information Theory to Security Engineering*. Cambridge University Press, 2011.
- [2] A. Mukherjee, S. A. A. Fakoorian, J. Huang, and A. L. Swindlehurst, "Principles of physical layer security in multiuser wireless networks: A survey," *IEEE Commun. Surveys Tuts.*, vol. 16, no. 3, pp. 1550–1573, 2014.
- [3] Y. Zou, J. Zhu, X. Wang, and L. Hanzo, "A survey on wireless security: Technical challenges, recent advances, and future trends," *Proc. IEEE*, vol. 104, no. 9, pp. 1727–1765, 2016.
- [4] A. B. Bash, D. Goeckel, and D. Towsley, "Limits of reliable communication with low probability of detection on AWGN channels," *IEEE J. Sel. Areas Commun.*, vol. 31, no. 9, pp. 1921–1930, Sep. 2013.
- [5] M. R. Bloch, "Covert communication over noisy channels: A resolvability perspective," *IEEE Trans. Inf. Theory*, vol. 62, no. 5, pp. 2334–2354, May 2016.
- [6] P. H. Che, M. Bakshi, C. Chan, and S. Jaggi, "Reliable deniable communication with channel uncertainty," in *Proc. IEEE Info. Theory Workshop (ITW)*, Hobart, TAS, Australia, Nov. 2014, pp. 30–34.
- [7] D. Goeckel, B. Bash, S. Guha, and T. D., "Covert communications when the warden does not know the background noise power," *IEEE Commun. Lett.*, vol. 22, no. 2, pp. 236 – 239, Feb. 2016.
- [8] B. He, S. Yan, X. Zhou, and V. K. Lau, "On covert communication with noise uncertainty," *IEEE Commun. Lett.*, vol. 21, no. 4, pp. 941–944, 2017.
- [9] M. Hayashi and Á. Vázquez-Castro, "Covert communication with Gaussian noise: from random access channel to point-to-point channel," *IEEE Trans. Commun.*, vol. 72, no. 3, pp. 1516–1531, 2023.
- [10] B. A. Bash, D. Goeckel, and D. Towsley, "Covert communication gains from adversary's ignorance of transmission time," *IEEE Trans. Wireless Commun.*, vol. 15, no. 12, pp. 8394–8405, 2016.
- [11] X. Lu, S. Yan, W. Yang, M. Li, and D. W. K. Ng, "Covert communication with time uncertainty in time-critical wireless networks," *IEEE Trans. Wireless Commun.*, vol. 22, no. 2, pp. 1116–1129, 2022.
- [12] T. V. Sobers, A. B. Bash, S. Guha, D. Towsley, and D. Goeckel, "Covert communication in the presence of an uninformed jammer," *IEEE Trans. Wireless Commun.*, vol. 16, no. 9, pp. 6193–6206, Sep. 2017.

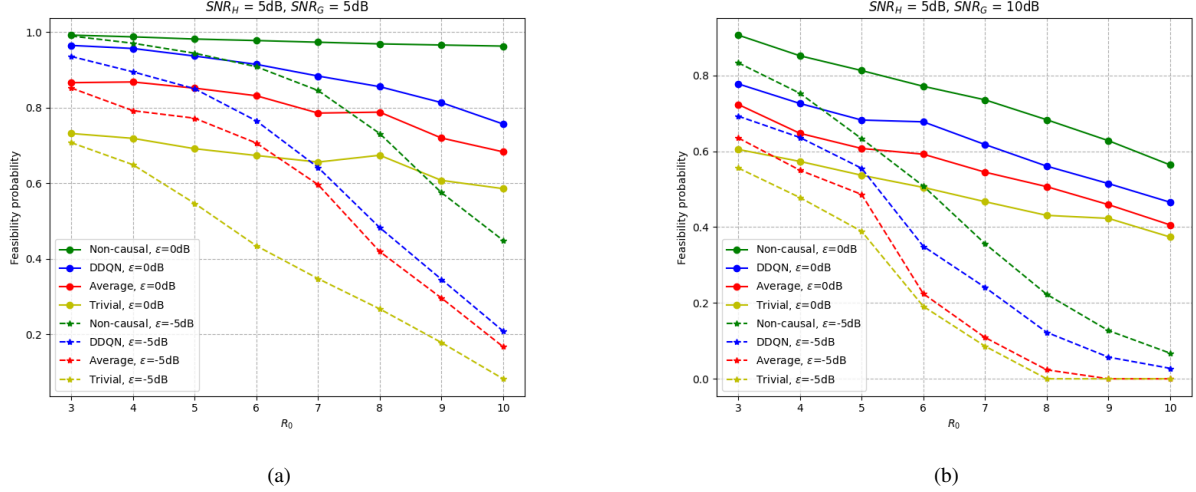


Fig. 9: Feasibility probabilities of causal rate allocation schemes.

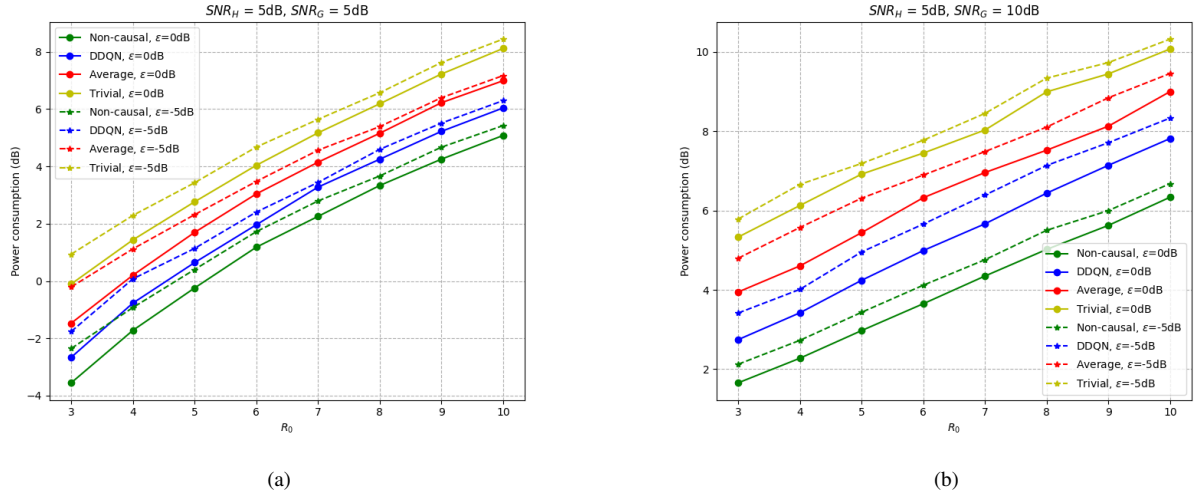


Fig. 10: Power consumptions under causal rate allocation schemes when they are all feasible.

- [13] H. ZivariFard, M. R. Bloch, and A. Nosratinia, "Covert communication in the presence of an uninformed, informed, and coordinated jammer," in *Proc. IEEE Int. Symp. on Info. Theory (ISIT)*, Melbourne, Australia, Jul. 2022, pp. 306–311.
- [14] —, "Covert communication via non-causal cribbing from a cooperative jammer," in *Proc. IEEE Int. Symp. on Info. Theory (ISIT)*, Melbourne, Australia, Jul. 2021, pp. 202–207.
- [15] S.-H. Lee, L. Wang, A. Khisti, and G. W. Wornell, "Covert communication with channel-state information at the transmitter," *IEEE Trans. Inf. Forensics Security*, vol. 13, no. 9, pp. 2310–2319, Sep. 2018.
- [16] H. ZivariFard, M. R. Bloch, and A. Nosratinia, "Keyless covert communication via channel state information," *IEEE Trans. Inf. Theory*, vol. 68, no. 8, pp. 5440–5474, Aug. 2022.
- [17] H. ZivariFard and X. Wang, "Covert communication via action-dependent states," *IEEE Trans. Inf. Theory*, vol. 71, no. 4, pp. 3100–3128, Apr. 2025.
- [18] A. Bendary, A. Abdelaziz, and C. E. Koksall, "Achieving positive covert capacity over MIMO AWGN channels," *IEEE J. Sel. Areas Inf. Theory*, vol. 2, no. 1, pp. 149–162, 2021.
- [19] K. Shahzad, X. Zhou, S. Yan, J. Hu, F. Shu, and J. Li, "Achieving covert wireless communications using a full-duplex receiver," *IEEE Trans. Wireless Commun.*, vol. 17, no. 12, pp. 8517–8530, 2018.
- [20] A. Sheikholeslami, M. Ghaderi, D. Towsley, B. A. Bash, S. Guha, and D. Goeckel, "Multi-hop routing in covert wireless networks," *IEEE Trans. Wireless Commun.*, vol. 17, no. 6, pp. 3656–3669, 2018.
- [21] J. Hu, S. Yan, X. Zhou, F. Shu, and J. Li, "Covert wireless communications with channel inversion power control in Rayleigh fading," *IEEE Trans. Veh. Technol.*, vol. 68, no. 12, pp. 12 135–12 149, 2019.
- [22] K. Shahzad and X. Zhou, "Covert wireless communications under quasi-static fading with channel uncertainty," *IEEE Trans. Inf. Forensics Security*, vol. 16, pp. 1104–1116, 2020.
- [23] J. Hu, S. Yan, X. Zhou, F. Shu, J. Li, and J. Wang, "Covert communication achieved by a greedy relay in wireless networks," *IEEE Trans. Wireless Commun.*, vol. 17, no. 7, pp. 4766–4779, 2018.
- [24] O. Shmuel, A. Cohen, and O. Gurewitz, "Multi-antenna jamming in covert communication," *IEEE Trans. Commun.*, vol. 69, no. 7, pp. 4644–4658, 2021.
- [25] J. Lee and N. Jindal, "Energy-efficient scheduling of delay constrained traffic over fading channels," *IEEE Trans. Wireless Commun.*, vol. 8, no. 4, pp. 1866–1875, 2008.
- [26] Y. Wang, S. Yan, W. Yang, Y. Huang, and C. Liu, "Energy-efficient covert communications for bistatic backscatter systems," *IEEE Transactions on Vehicular Technology*, vol. 70, no. 3, pp. 2906–2911, 2021.
- [27] E. L. Lehmann and J. P. Romano, *Testing Statistical Hypotheses*. New York, NY, USA: Springer-Verlag, 2005.
- [28] M. Mohri and A. Rostamizadeh, *Foundations of machine learning*. Cambridge, Massachusetts: The MIT Press, 2018.
- [29] A. Chorti, K. Papadaki, and H. V. Poor, "Optimal power allocation in block fading channels with confidential messages," *IEEE Trans. Wireless Commun.*, vol. 14, no. 9, pp. 4708–4719, 2015.